Translational Oncology
www.transonc.com

Volume 12 Number 1 January 2019 pp. 49–61 49

Vimentin and Non-Muscle Myosin IIA are Members of the Neural Precursor Cell Expressed Developmentally Down-Regulated 9 (NEDD9) Interactome in Head and Neck Squamous Cell Carcinoma Cells[1]

Martina Semelakova[*,†,2], Stèphane Grauzam[†,2], Prabhakar Betadthunga[†,‡], Jessica Tiedeken[†], Sonya Coaxum[†,§], David M. Neskey[†,§,¶] and Steven A. Rosenzweig[†,¶]

[*]Institute of Biology and Ecology, Department of Cell Biology, Faculty of Science, Pavol Jozef Šafárik University, Košice, Slovakia; [†]Department of Cell and Molecular Pharmacology & Experimental Therapeutics, Medical University of South Carolina, 173 Ashley Avenue MSC 509, Charleston, SC 29425-5050; [‡]Department of Post Graduate-Studies and Research in Biotechnology, Sahydri Science College, Kuvempu University, Shimoga, Karnataka, India, 577203; [§]Department of Otolaryngology, Head and Neck Surgery, Medical University of South Carolina; [¶]Hollings Cancer Center, Medical University of South Carolina, 173 Ashley Avenue MSC 550, Charleston, SC 29425-5050

Abstract

Here we demonstrate an interaction between neural precursor cell expressed, developmentally-downregulated 9 (NEDD9) and the cytoskeletal proteins vimentin and non-muscle myosin IIA (NMIIA), based on co-immunoprecipitation and mass spectrometric sequence identification. Vimentin was constitutively phosphorylated at Ser56 but vimentin associated with NEDD9-was not phosphorylated at Ser56. In contrast, NMIIA bound to NEDD9 was phosphorylated on S1943 consistent with its function in invasion and secretion. Treatment of cells with the vimentin-targeting steroidal lactone withaferin A had no effect on vimentin turnover as previously reported, instead causing NEDD9 cleavage and cell death. The NMIIA-selective inhibitor blebbistatin induced cells to form long extensions and attenuated secretion of matrix metalloproteinases (MMPs) 2 and 9. While the site of vimentin interaction on NEDD9 was not defined, NMIIA was found to interact with NEDD9 at its substrate domain. NEDD9 interactions with vimentin and NMIIA are consistent with these proteins having roles in MMP secretion and cell invasion. These findings suggest that a better understanding of NEDD9 signaling is likely to reveal novel therapeutic targets for the prevention of invasion and metastasis.

Translational Oncology (2019) 12, 49–61

Introduction

Tumor cell invasion and metastasis to distant organ sites represents the primary cause of mortality and morbidity for most cancer patients. In particular, metastasis is the final step leading to patient death from most solid tumors, including head and neck squamous cell carcinoma (HNSCC). Overexpression of Neural precursor cell expressed developmentally downregulated 9 (NEDD9) is associated with increased invasion and metastasis in multiple cancer sites and a mouse model of melanoma [1]. Indeed, it has been suggeested that elevated NEDD9 expression levels may serve as a biomarker for tumor aggressiveness [2]. Consistent with this view, we [3]

Address all correspondence to: Steven A. Rosenzweig, Department of Cell and Molecular Pharmacology & Experimental Therapeutics, Medical University of South Carolina MSC 509, 173 Ashley Avenue, Charleston, SC 29425. E-mail: rosenzsa@musc.edu

[1] Disclosure of Potential Conflicts of Interest: The authors have no conflicts of interest to declare.

[2] These two authors made equal contributions to this manuscript.

Received 4 September 2018; Revised 8 September 2018; Accepted 8 September 2018

1936-5233/19
https://doi.org/10.1016/j.tranon.2018.09.006

demonstrated that NEDD9 is a key regulator of invasive behavior in HNSCC cell lines, and others have shown that NEDD9 is expressed in the most invasive human head and neck squamous cell carcinoma (HNSCC) tumor specimens [4]. NEDD9 was also shown to be overexpressed in cervical cancer [5] where NEDD9 promotes migration and invasion attributable to a positive feedback loop of NEDD9 tyrosine phosphorylation downstream of Src activation and secondarily to focal adhesion kinase (FAK) [5,6].

NEDD9 is a member of the Cas family of scaffold proteins comprised of an N-terminal SH3 domain, a substrate domain containing multiple YxxP motifs for tyrosine phosphorylation for SH2-domain containing protein association, a serine-rich domain and a C-terminal helix-loop-helix motif. A goal of our work is to define NEDD9 signaling pathways that contribute to invasion in HNSCC cells. To determine the molecular details of NEDD9 protein interactions leading to invasion, we generated and analyzed a series of NEDD9 mutants with the results of these studies revealing that substrate domain tyrosine phosphorylation and an intact SH3 domain are essential for NEDD9 mediated matrix metalloproteinase-9 (MMP9) secretion and invadopodia formation [6].

As a function of the invasive process, tumor cells undergo epithelial to mesenchymal transition (EMT), an important biological process during development and oncogenesis [7,8]. The resulting down-regulation of E-cadherin and increased expression of the mesenchymal marker vimentin are considered hallmarks of this transition [9,10]. In head and neck squamous cell carcinoma (HNSCC), β-catenin and E-cadherin are down-regulated along with increased aberrant expression of vimentin [11]. Vimentin, a member of the type III intermediate filament family of proteins, is ubiquitously expressed in normal mesenchymal cells [12] and has been detected in HNSCC patient tumors and cell lines [13,14]. Elevated vimentin expression occurs in various epithelial cancers including prostate cancer, gastrointestinal tumors, CNS tumors, breast cancer, malignant melanoma, and lung cancer among others, and correlates with increased tumor growth, invasion and poor prognosis [15]. Vimentin has also been shown to alter mitochondrial membrane potential and the motility of mitochondria [16]. NEDD9 may regulate vimentin and E-cadherin expression, in turn modulating cell migration and invasion in cervical cancer cells as they become more stem-like [5].

Non-muscle myosin IIs (NMIIs) are ATP-driven molecular motors comprising an essential part of the motile machinery of eukaryotic cells. Cell migration requires coordinated formation of focal adhesions (FAs) and assembly and contraction of the actin cytoskeleton. NMIIs are critical mediators of contractility and focal adhesion dynamics in cell migration. Members of the NMII family catalyze the conversion of chemical energy into directed movement and force acting as regulators of the cytoskeleton. NMII isoforms promote cytoskeletal force generation in established cellular processes like cell migration, shape changes, adhesion dynamics, endocytosis, exocytosis and cytokinesis [17]. NMII defines three distinct isoforms in vertebrates; NMIIA, NMIIB and NMIIC [18,19], each heavy chain being encoded by a different gene, MYH9, MYH10 and MYH14, respectively, located on three different chromosomes [20–23]. The myosins constitute a large and diverse superfamily of motor proteins that bind actin filaments to produce force and tension. NMIIA Ser1916 phosphorylation is increased during TGF-β-induced EMT and results in FA formation and NMIIA association with FAs [19]. NMIIA Ser1943 phosphorylation is upregulated during integrin engagement with fibronectin. Of note, NMIIA is required for invasion [24] with S1943 phosphorylation potentially regulating the ability of NMIIA to mediate the invasive phenotype [25].

The objective of this study was to identify proteins interacting with NEDD9 in HNSCC cells. To that end, we identified vimentin and NMIIA as novel NEDD9 interacting proteins. Vimentin is known to contribute to cellular architecture, EMT [26], vesicular trafficking (endocytosis and secretion), invasion, invadopodia structure [27], and pseudopodia formation [28]. NMIIA has been shown to interact with Rab6 to regulate vesicle trafficking between the ER and Golgi [29,30], to participate in mechanosensing during cell migration [18,19] and to function as a tumor suppressor [31,32]. On this basis, both of these proteis may collaborate with NEDD9 to modulate the invasive, metastatic process.

Materials and Methods

Tissue Culture

Human HNSCC cell lines SCC9, SCC25 and FaDuwere obtained from American Type Culture Collection (ATCC, Manassas, USA). UMSCC22A/B cells representing a primary tumor from the hypopharynx (UMSCC22A) and its metastasis (UMSCC22B) [33] cells were from Dr. Tom Carey, University of Michigan Department of Otolaryngology, University of Michigan. Cells were cultured in Dulbecco's modified Eagle's medium (DMEM; GIBCO, USA) containing 10% fetal bovine serum (FBS) in a humidified atmosphere of 5% CO_2 at 37 °C. For all experiments, cells were seeded in 100 cm dishes, grown overnight to 50% to 70% confluency, and serum starved for 24 h before the treatment.

Preparation of NEDD9 Mutants

NEDD9 mutants were prepared as described previously [6]. The primers were prepared by PCR using TURBO DNA Polymerase (Stratagene) and digestion with *Dpn*I. DH5α competent cells were transformed with mutant PCR products by heat shock at 42°C/30 s and transformants were incubated at 37°C/1 h with SOC medium and then incubated on LB agarose plates at 37°C overnight with kanamycin (50μg/μl), followed by cDNA isolation (Maxiprep cDNA Kit, Qiagen). The positive mutant sequences were identified using GenBank database sequences.

Transfection of Cells

Cells were transfected using NanoJuice transfection reagent according to the manufacturer's protocol. Cells were quickly resuspended in medium containing 10% FBS and allowed to recover. A total of 5×10^4 cells were seeded into each well of a 6-well plate. The cells were collected 24 h after transfection.

shRNA Transduction/Gene Silencing

Cells were seeded in 6 cm plates prior to shRNA transduction according to the manufacturer's standard protocol using pLKO.1 - TRC Cloning Vector from Addgene (USA), Addgene Plasmid 10878. shRNAs (Sigma MISSION) were obtained from The Hollings Cancer Center shRNA Repository/Shared Resource.

Immunoprecipitation and Immunoblot Analysis

Cells were washed with ice-cold PBS and harvested in ice-cold cell lysis buffer containing protease and phosphatase inhibitors by scraping. Lysates were centrifuged at 10,000×*g* for 10 min and the supernatants were used for protein measurement (Pierce BCA Protein

Assay Kit, Thermo Scientific). Five micrograms of total protein from each sample was resolved on a 10% acrylamide SDS gel. For immunoprecipitation, cells were disrupted in 250 µl of immunoprecipitation buffer. Equal amounts of protein (300 µg) were subjected to immunoprecipitation followed by Western blot analysis. Primary antibodies used were: NEDD9 (ab18056, Abcam), Vimentin (RV202: sc-32322 mouse monoclonal antibody, Santa Cruz), Vimentin (D21H3, XP Rabbit mAb, Cell Signaling) and β-actin (sc-1616-R, Santa Cruz). In some cases immunopreciptation was carried out using anti-GFP bound to beads (GFP-Trap-A, Chromotek. Proteins were separated on SDS gels, transferred to membranes, and probed with the vimentin (RV202: sc-32322), or actin and appropriate secondary antibodies. Bands were visualized using an ECL Kit (Pierce, USA). The analysis of cell fractions (cytoplasmic or nuclear) was performed according to a standard protocol [34].

Immunocytochemistry/Confocal Microscopy

Human HNSCC cells were incubated with primary antibody o/n, followed by 2h incubation with Alexa Fluor 647 fluorescent dye-conjugated sec. antibody, Hoechst 3334, TRITC, stained with Rhodamine-Phalloidin and analysed on Olympus FV10i laser scanning confocal microscope. Images of Vimentin (400×) were captured by confocal microscopy (Olympus) using Olympus Imaging Software 2.6.

Gelatin Zymography

Secreted MMPs in conditioned medium were affinity adsorbed with gelatin-Sepharose as previously detailed [3,6]. SDS sample buffer lacking DTT was added and proteins were resolved on 10% acrylamide, SDS gels containing polymerized gelatin (0.5-2 mg/ml). MMPs were renatured using two 30 min detergent exchange washes. Gels were incubated for 6-48 h at 23°C to allow MMPs to degrade the gelatin followed by staining with Coomassie brilliant blue. Destained gels were scanned and inverse images were quantified using ImageJ, with relative absorbance values for MMP9 or MMP2 normalized to cell lysate actin ratios.

LC/MS/MS Analysis: Sample Preparation

Following GFP immunoprecipitation and gel electrophoresis, gel bands of interest were excised from the the gels and washed with 50 mM ammonium bicarbonate for 10 min. Next, the bands were destained using 25 mM ammonium bicarbonate in 50% acetonitrile for 15 min, repeated twice. Bands were then reduced with DTT and alkylated with 55 mM Iodoacetamide (Sigma). The gel bands were next washed with 50 mM ammonium bicarbonate for 10 min, followed by dehydration with 100% acetonitrile for 15 mi and drying in a speedvac. Each gel band was covered with proteomics grade trypsin (Sigma) and incubated at 37C overnight. Supernatants were collected in clean dry tubes and peptides were further extracted with one wash of 25mM ammonium bicarbonate for 20 min and three washes of 5% formic acid, containing 50% acetonitrile for 20 min each. Supernatant were collected and pooled after each wash then dried down in a speedvac to ~1 µl. Samples were reconstituted in 7 µl of mobile phase A (95% water, 5% acetonitrile and 0.2% formic acid) and placed in autosampler vials.

LC MS/MS Analysis: Orbitrap Elite w/ETD

Peptides were separated with a linear gradient of 5–50% buffer B (95% ACN and 0.2% formic acid) at a flow rate of 200 nL/min on a C18-reversed phase column (75 mm × 15 cm) packed in-house with Waters YMC-ODS C18-AQ 5 mm resin. A Dionex U3000 nano-LC chromatography system (ThermoFisher Scientific) was coupled on-line to an Orbitrap Elite instrument (ThermoFisher Scientific) via a Nanospray Flex Ion Source (ThermoFisher Scientific). MS data was acquired with a data-dependent strategy selecting the fragmentation events based on the precursor abundance in the survey scan (400-1700 Th). The resolution of the survey scan was 60,000 at *m/z* 400 Th with a target value of 1e6 ions and 1 microscan. Low resolution CID MS/MS spectra were acquired with a target value of 5000 ions in normal CID scan mode. MS/MS acquisition in the linear ion trap was partially carried out in parallel to the survey scan in the Orbitrap analyzer by using the preview mode (first 192 ms of the MS transient). The maximum injection time for MS/MS was 100 ms. Dynamic exclusion was 120 s and early expiration was enabled. The isolation window for MS/MS fragmentation was set to 2.

Database Searching and Quantification

Raw data were searched with Proteome Discoverer 1.4 using the Human IPI v3.72 database. Static modification of carbomidomethyl on cysteines and variable modifications of methionine oxidation and Phosphorylation of serine, threonine, and tyrosine were included. Protein identifications must have an Xcorr *vs.* charge state >1.5, 2.0, 2.5 for +1, +2, and +3 ions, with at least 2 unique peptides matching the protein and a good match for at least 4 consecutive y or b ion series from the MS/MS spectra.

Results

Vimentin is a NEDD9-Interacting Protein

We previously reported that IGF-1 induced VEGF secretion results in autocrine VEGF action in HNSCC cells [35]. This led to a phosphotyrosine proteomics analysis resulting in the identification of NEDD9 (human enhancer of filamentation, HEF1; Crk-associated substrate in lymphocytes, Cas-L) as a tyrosine phosphorylated effector protein downstream of VEGF action in HNSCC cells, where it functions as a key regulator of motility and invasion [3]. To further define the NEDD9 interactome and identify additional proteins that may contribute to the invasive phenotype, we screened for NEDD9 interacting proteins following EGFP-NEDD9 immunoprecipitation from SCC9 cells stably expressing EGFP-tagged NEDD9 [6] followed by SDS gel resolution and band identification by by mass spectrometry. As shown in Figure 1*A*, a major protein identified by mass spectrometry was vimentin. Vimentin is a 55 kDa cytoplasmic protein expressed in many cell types, predominantly those of mesenchymal origin [36,37]. Based on its being a type III intermediate filament protein, it is generally accepted that vimentin functions as a structural protein maintaining cellular architecture, along with being a marker of EMT [15,38,39]. We identified approximately 45% of the vimentin sequence (Figure 1*B*) and noted the lack of Ser56 phosphorylation (underlined) in the 13 residue tryptic peptide, SLYASSPGGVYATR (residues 51-64; Figure 1, *A* or *B*).

To confirm the NEDD9-vimentin interaction, we carried out direct immunoprecipitation studies with anti-NEDD9 antibodies. As shown in Figure 2*A*, vimentin is expressed in cells derived from a HNSCC metastasis, UMSCC22B cells, but not in cells derived from the primary tumor, UMSCC22A cells. Differences in the electropboretic mobility of NEDD9 between UMSCC2A and UMSCC2B cell lines, reflect its differential phosphorylation [40]. In Figure 2*B*, vimentin co-immunoprecipitated along with NEDD9 in SCC9 cell

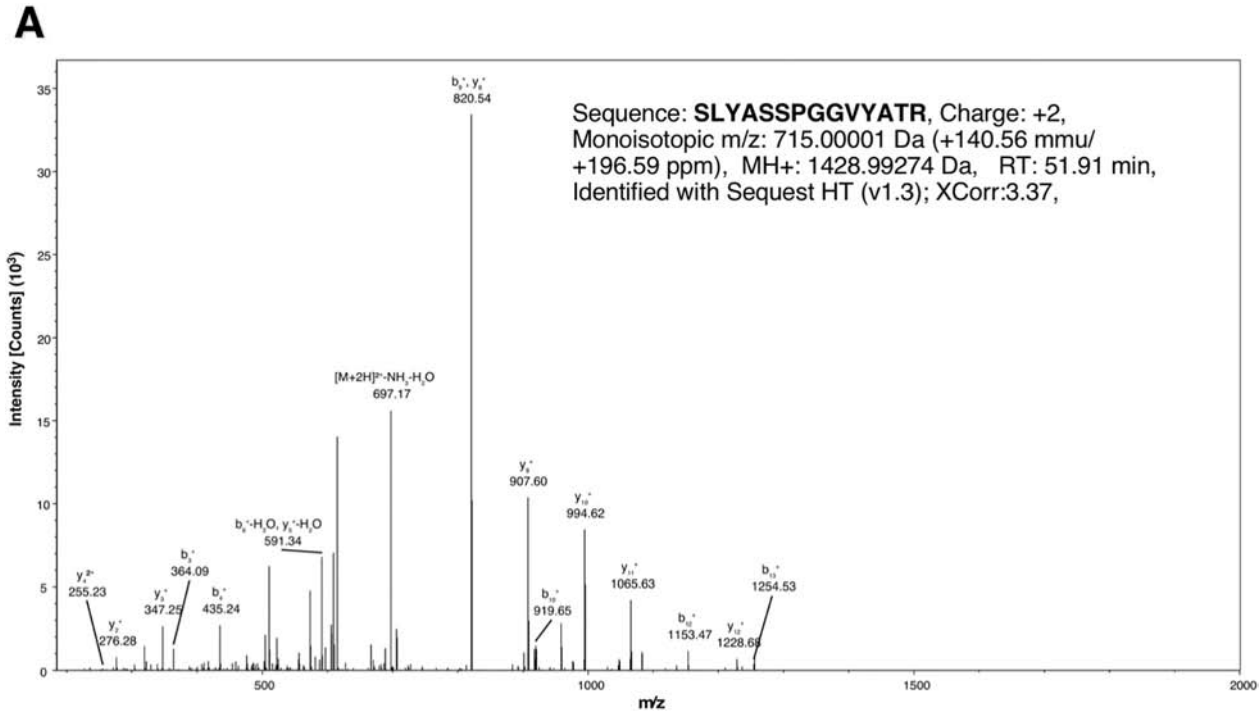

B

```
        10         20         30         40         50
MSTRSVSSSS YRRMFGGPGT ASRPSSSRSY VTTSTRTYSL GSALRPSTSR
        60         70         80         90        100
SLYASSPGGV YATRSSAVRL RSSVPGVRLL QDSVDFSLAD AINTEFKNTR
       110        120        130        140        150
TNEKVELQEL NDRFANYIDK VRFLEQQNKI LLAELEQLKG QGKSRLGDLY
       160        170        180        190        200
EEEMRELRRQ VDQLTNDKAR VEVERDNLAE DIMRLREKLQ EEMLQREEAE
       210        220        230        240        250
NTLQSFRQDV DNASLARLDL ERKVESLQEE IAFLKKLHEE EIQELQAQIQ
       260        270        280        290        300
EQHVQIDVDV SKPDLTAALR DVRQQYESVA AKNLQEAEEW YKSKFADLSE
       310        320        330        340        350
AANRNNDALR QAKQESTEYR RQVQSLTCEV DALKGTNESL ERQMREMEEN
       360        370        380        390        400
FAVEAANYQD TIGRLQDEIQ NMKEEMARHL REYQDLLNVK MALDIEIATY
       410        420        430        440        450
RKLLEGEESR ISLPLPNFSS LNLRETNLDS LPLVDTHSKR TLLIKTVETR
       460
DGQVINETSQ HHDDLE
```

Figure 1. Identification of vimentin as a NEDD9 interacting protein. A) Analysis of EGFP-NEDD9 immunoprecipitates by mass spectrometry revealed the presence of vimentin. B) Primary sequence of vimentin with Ser56, a common site of phosphorylation in vimentin, shown in red [46,47,61]. Vimentin present in NEDD9 co-immunoprecipitates was not phosphorylated on Ser56. Based on the peptides identified, 45% of the vimentin sequence was covered in these experiments and is shown in blue.

extracts and not in UMSCC22A cells, which lack vimentin expression. Also shown in Figure 2*B*, vimentin co-immunoprecipitated along with the monooxygenase containing, NEDD9 interacting protein MICAL1 (molecule interacting with Cas-L1, [41]) in SCC9 cells. Based on microscopy, vimentin was primarily localized within a perinuclear fibrillar nework in SCC9 cells (Figure 2*D*) consistent wwith its co-immunoprecipitation with NEDD9 from the cytoskeletal fraction (Figure 2*C*). Intermediate filament proteins such as vimentin localize to the perimuclear space associating with nuclear structures resulting in their fractionation with nuclear proteins [42]. Vimentin localization in UMSCC2B cells was similar to that seen in SCC9 cells with additional punctate staining within the cytoplasm (Figure 2*D*).

Withaferin A (WFA) Treatment Depletes NEDD9 Levels

We next tested the effect of the small molecule plant steroidal lactone, withaferin A (WFA) on SCC9 cells. Treatment of cells with WFA has been reported to cause the selective cleavage of vimentin [43]. As shown in Figure 3*A*, treatment with 5 μM WFA for 24 h had a negligible effect on vimentin stability or expression. Instead, NEDD9 was cleaved (Figure 3, *A* and *C*). NEDD9 is a known

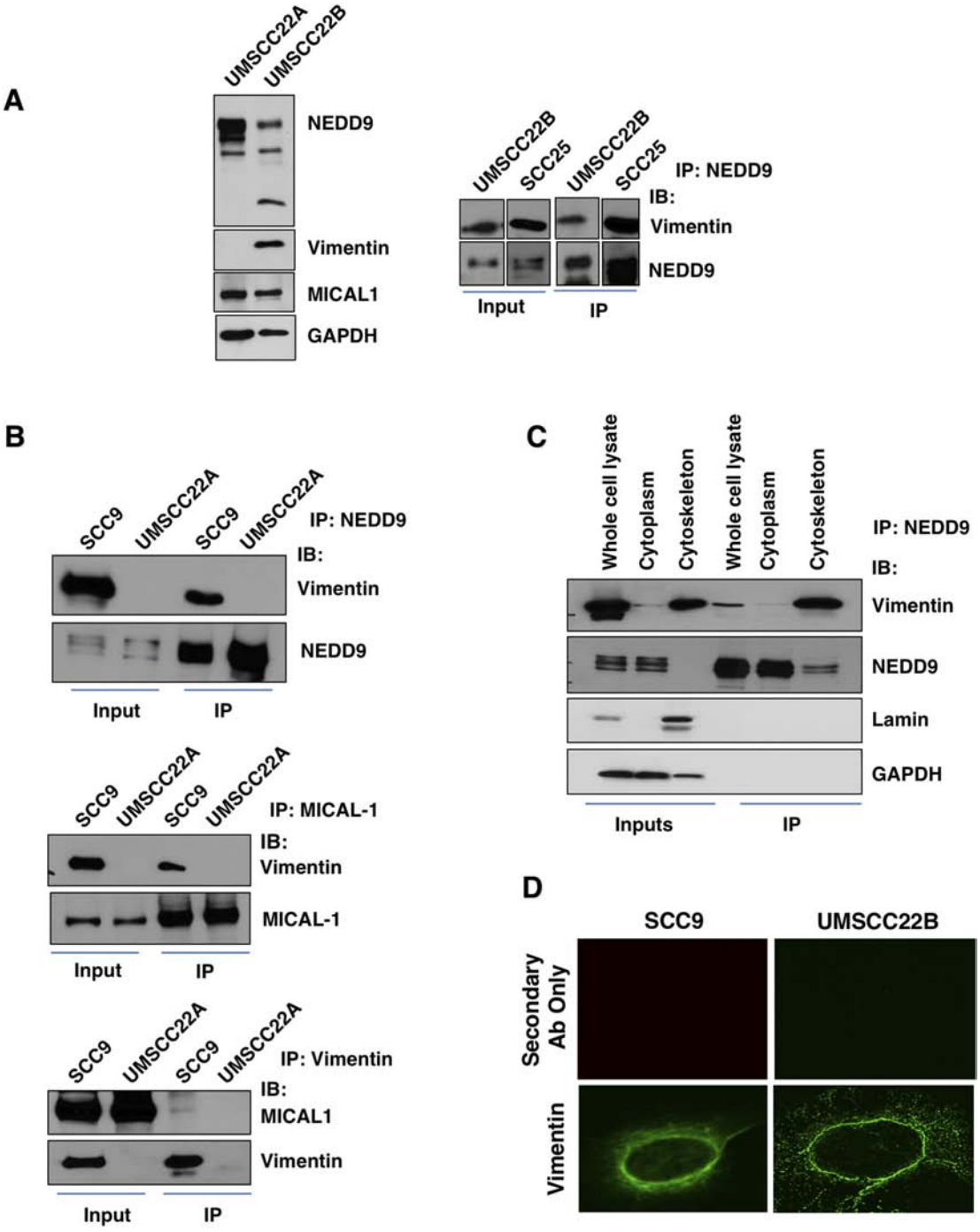

Figure 2. Validation of the interaction between NEDD9 and vimentin. A) (*Left*), UMSCC22A and UMSCC22B were immunoblotted for NEDD9, vimentin, MICAL1 and GAPDH. UMSCC22A cells, isolated from a primary tumor of the tongue, lack vimentin expression whereas UMSCC22B cells, derived from a metastasis in the same patient, exhibit vimentin expression. NEDD9 and the NEDD9 and vimentin interacting protein MICAL1 [41] were expressed in both cell lines. (*Right*), Vimentin co-immunoprecipitates with NEDD9 in UMSCC22B and SCC25 cells. B) Vimentin co-immunoprecipitates with NEDD9 in SCC9 cells, but not in UMSCC22A cells which lack vimentin expression. Vimentin co-immunoprecipitates with the NEDD9-interacting protein MICAL1 in SCC9 cells [6]. C) Fractionation of SCC9 cells demonstrates that vimentin preferentially associates with the nuclear/cytoskeletal fraction where it associates with NEDD9. D) Confocal microscopy confirms the perinuclear and cytoplasmic distribution of vimentin.

caspase substrate with two caspase cleavage sites in its sequence (Figure 3*B*), one of which in turn, generates the proapoptotic C-terminal fragment (residues 631-834) [44]. As shown in Figure 3*C* (lower), vimentin levels were unchanged over a dose range of 1-5 μM WFA, whereas NEDD9 levels exhibited a dose-dependent decrease as a function of increasing doses of WFA. Examination of SCC9 cells by light microscopy revealed that WFA treatment induced cell death/apoptosis in response to WFA (Figure 3*C* upper). The loss of MMP9/MMP2 secretion is a reflection of NEDD9 loss [6] and cell death.

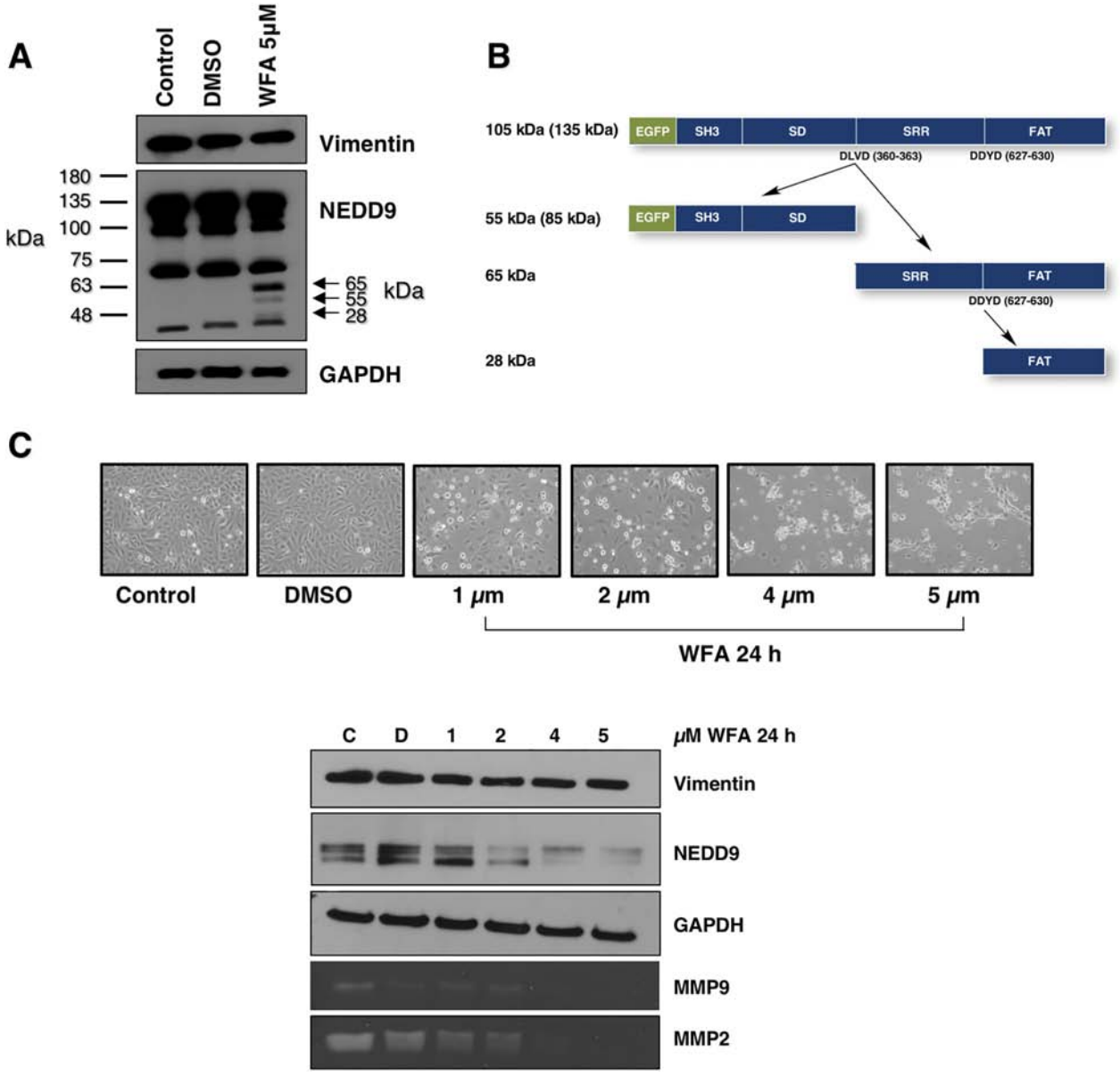

Figure 3. Withaferin-A (WFA) treatment results in NEDD9 cleavage and cell death. A). Immunoblot of control, DMSO and WFA (5 μM) treated SCC9 cells. B) NEDD9 structure showing location of its caspase cleavage sites DLVD and DDYD. C) Dose-dependent change in SCC9 cell morphology (*upper*) in response to WFA treatment and cleavage of NEDD9 (*lower*). The WFA-induced loss of NEDD9 via caspase cleavage is consistent with apoptotic cell death. Also shown is loss of MMP9/2 secretion in response to WFA treatment, reflecting cell death.

Vimentin Undergoes Regulated Phosphorylation on Ser38

A variety of kinases phosphorylate vimentin on serine residues, with Ser56 being a key phosphorylation site present within the head region of vimentin (Figure 4*A*); a domain through which vimentin binds to the NEDD9 paralog, p130Cas (breast cancer anti-estrogen resistance 1; BCAR1) [45]. Of note, the vimentin-p130Cas interaction is disrupted by Ser56 phosphorylation of vimentin, releasing bound p130Cas [46,47]. We found that Ser56 was constitutively phosphorylated in SCC9 cells (Figure 4*B*). On the other hand, Ser38 phosphorylation was induced by serum, EGF and IGF1 treatment (Figure 4, *C–E*). Consistent with the structural similarities between p130Cas and NEDD9, the binding of NEDD9 to vimentin lacking a Ser56 phosphate would be expected. This is consistent with our mass spectrometry findings, suggesting that immunoprecipitated vimentin bound to EGFP-NEDD9 is not phosphorylated on Ser56 (Figure 1).

Non-Muscle Myosin IIA (NMIIA) is a NEDD9-Interacting Protein

In addition to vimentin, we also identified non-muscle myosin IIA (NMIIA; Myh9) as a NEDD9 interacting protein (Figure 5). NMIIA is expressed by most eukaryotic cell types and is an actin motor protein involved in cytokinesis, cell motility and cell shape, secretion and cell polarity [18]. As noted in Figure 5, d NMIIA bound to NEDD9 was phosphorylated on Ser1943. NMIIA contains a number of phosphorylation sites within its C-terminal tailpiece [25]. Ser1943 is present in the non-helical tail region of NMIIA (residues 1928-1960) and its phosphorylation controls the intracellular localization of

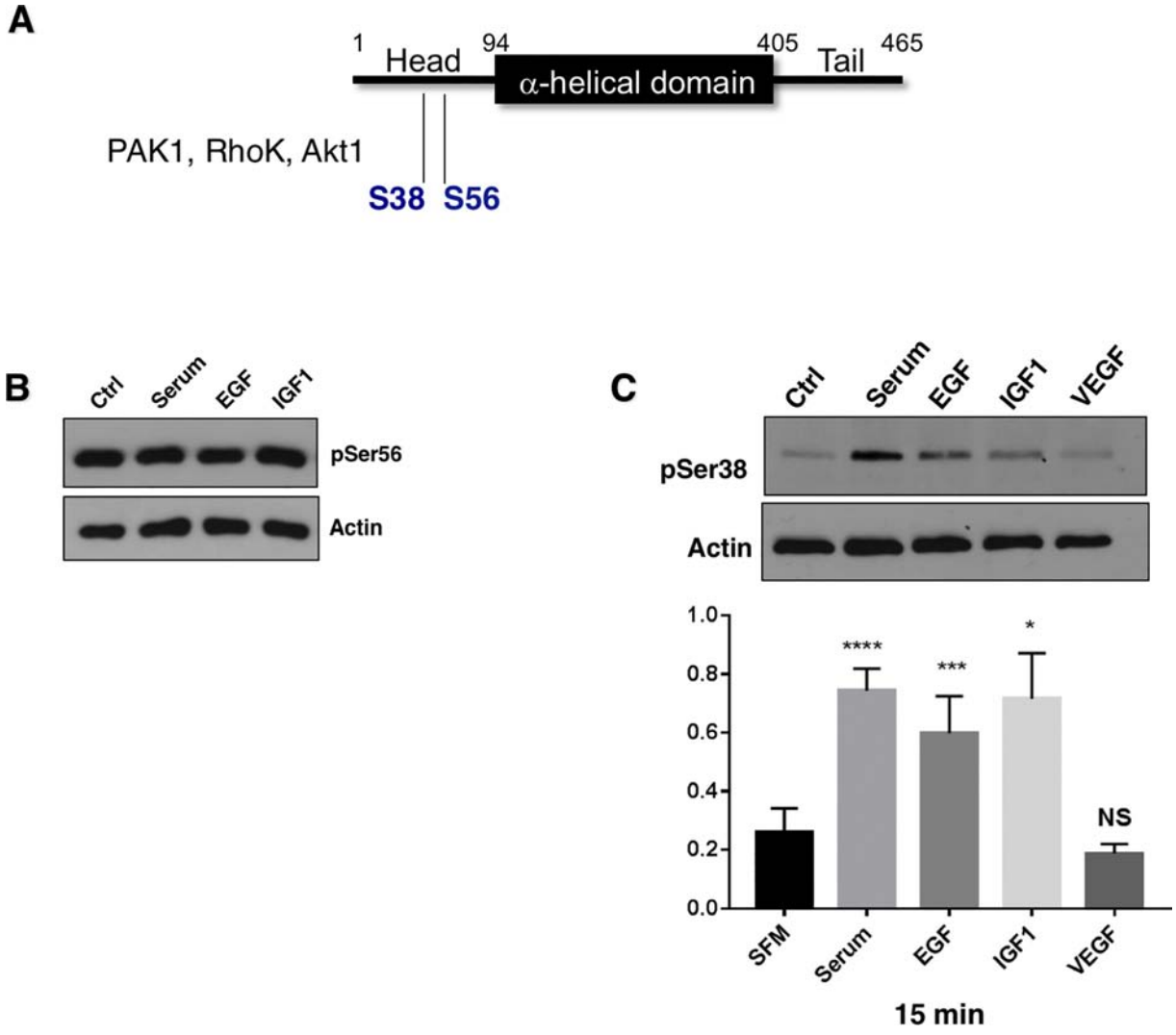

Figure 4. Vimentin is a phosphoprotein. A) Schematic of vimentin structure delineating its head, α-helical and tail domains [45,67]. The head domain is the principal site of of phosphorylation by a number of kinases, which in turn, regulates vimentin filament assembly/disassembly. Ser56 phosphorylation causes disassociatiuon of the NEDD9 paralog, p130Cas from vimentin [46,47]. B) Ser56 phosphorylation of vimentin in control and growth factor treated SCC9 cells. C-E) Ser38 phsophorylation of vimentin in response to growth factor treatment with quantification of the response to growth factors.

NMIIA including its binding to the Golgi complex and to secretory vesicles via glycosyl transferases and Rab6A [48].

Validation of an NMIIA-NEDD9 Interaction and Identification of the NMIIA Site of Interaction on NEDD9

Using a panel of NEDD9 truncation and tyrosine mutants recently evaluated for their abilities to affect MMP9 secretion and invadopodia formation [6], we tested whether we could identify the site of NMIIA interaction on NEDD9. As shown in Figure 6A, NMIIA was immunoprecipitated from SCC9 cells stably expressing the EGFP-tagged mutants indicated and the washed precipitates were resolved on 10% acrylamide SDS gels, followed by transfer and immunoblotting with anti-GFP antibodies. For the NEDD9 constructs tested, WT, ΔSH3 (deleted SH3 domain), ΔCT (deleted C-terminal/FAT domain), SS (substrate domain and SRR, Serine Rich Region), we identified an EGFP band migrating at the appropriate position in the gel, as noted by a red dot to the left of the lane. However, in the case of F13NEDD9, in which all 13 tyrosine residues present in a YxxP motif within the substrate domain (SD), are replaced with phenyalanines (F)), an EGFP-tagged band was not detected. This was not due to a lack of F13NEDD9 expression based on our use of a portion of the whole cell lysate from F13NEDD9 expressing cells as input in the first lane. Based on this, we concluded that NMIIA binding to NEDD9 requires tyrosine phosphorylation of one or more SD tyrosines. It is uncertain whether this is a direct interaction between NMIIA and NEDD9 or if it occurs via an intermediary protein that binds to NEDD9 phosphotyrosine(s). Using proximity ligation analysis, which we previously used to identify NEDD9 protein:protein interactions in intact cells [6], we noted that NEDD9-NMIIA complexes are detectable in cells (Figure 6*B*).

NMIIA is Expressed in All HNSCC Cell Lines Examined, Localizing to the Cytoplasm and Perinuclear Space

We next evaluated a panel of HNSCC cell lines for NMIIA and NEDD9 expression. As expected, NMIIA was present in all cell lines tested, as was NEDD9 (Figure 7*A*). SCC9 and UMSCC22A cells

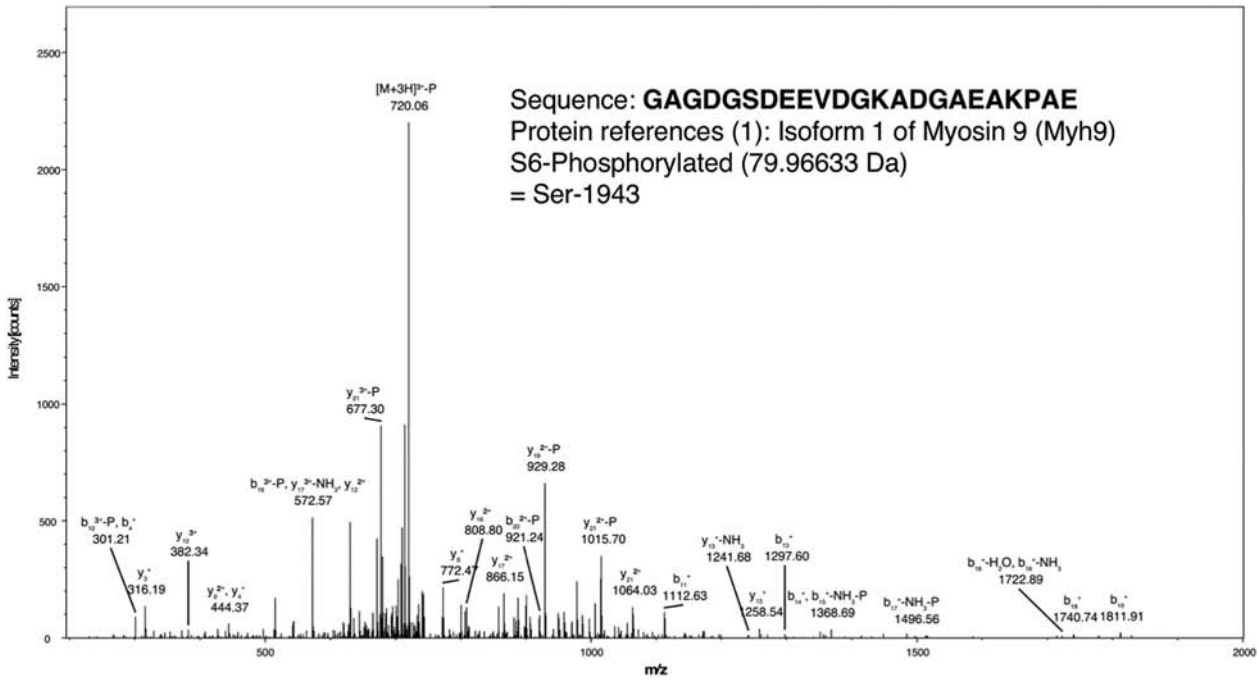

Figure 5. Identification of NMIIA as a NEDD9 interacting protein. A) Analysis of EGFP-NEDD9 immunoprecipitates by mass spectrometry revealed NMIIA as a NEDD9 binding partner. Ser1943 of NMIIA was found to be phosphorylated consistent with its role in regulating NMIIA localization and filament assembly [48,68].

were next separated into nuclear (N) and cytoplasmic (C) fractions prior to immunoblotting for NMIIA. NMIIA has recently been described as a tumor suppressor that functions, in part, by retaining p53 in the nucleus [31,32]. As shown in Figure 7*B*, NMIIA was present in both the nuclear (includes cytoskeleton) and cytoplasmic fractions. Treatment of UMSCC22A cells with the NMIIA selective ATPase inhibitor blebbistatin reduced level of NMIIA within the nucleus (cytoskeleton), although we did not observe a commensurate

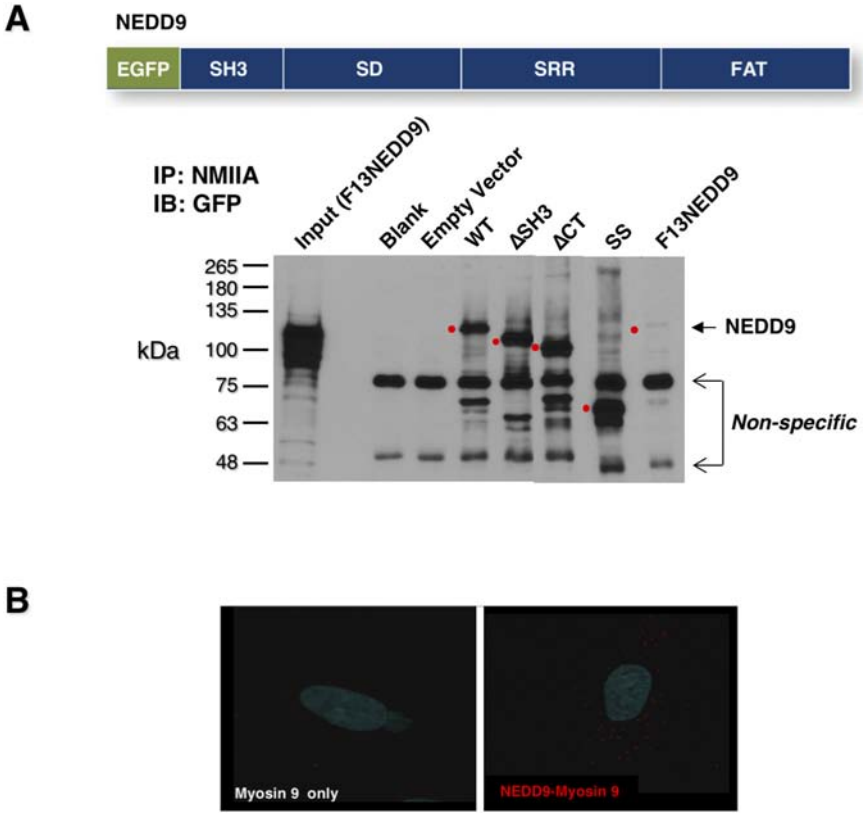

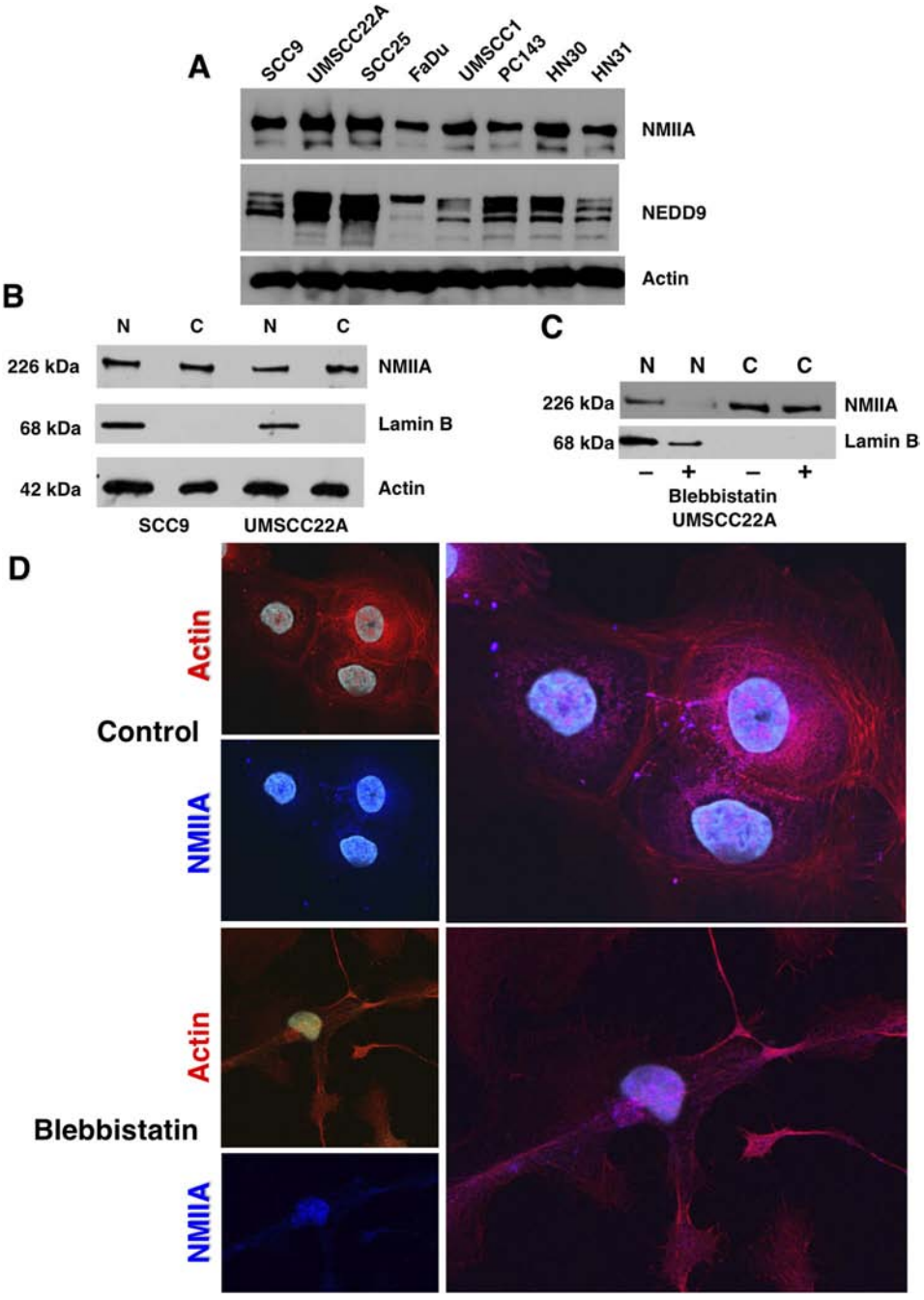

Figure 7. NMIIA expression in HNSCC cell lines and presence in the cytoskeletal fraction. A) NMIIA expressed in HNSCC cell lines. B) NMIIA is present in nuclear and cytoplasmic fractions. C) Treatment of cells with blebbistatin decreases the association of NMIIA with the nuclear/cytoplasmic fraction. D) Confocal microscopy of control and blebbistatin-treated SCC9 cells.

increase in the cytoplasm as previously reported [31,32] suggesting it may have been degraded (Figure 7*C*). Immunocytochemical staining of control and blebbistatin treated SCC9 cells showed a similar distribution of NMIIA before and after blebbistatin treatment (Figure 7*D*). These images show that NMIIA inhibition with blebbistatin induces in the formation of long, narrow extensions (Figure 7*D*) which has been

Figure 6. Inability of substrate domain to bec phosphorylated eliminates NMIIA-NEDD9 binding interaction. NMIIA was immunoprecipitated from a panel of cell lines stably expressing the EGFP-tagged NEDD9 mutants indicated. The presence of NEDD9 in the immunoprecipitates was evaluated by immunoblotting with antii-GFP antibodies. Shown in the upper image is the structure of NEDD9 with each of its domains indicated; SH3 domain (SH3), substrate domain (SD), serine-rich region (SRR) and C-terminal focal adhesion targeting domain (FAT). The lower image is a representative gel demonstrating the results of NMIIA immunoprecipitation followed by GFP immunoblot. The red dots depict the migration position of the NEDD9 mutant being blotted. Also evident are two non-specific bands also detected in the blank and empy vector control lanes.

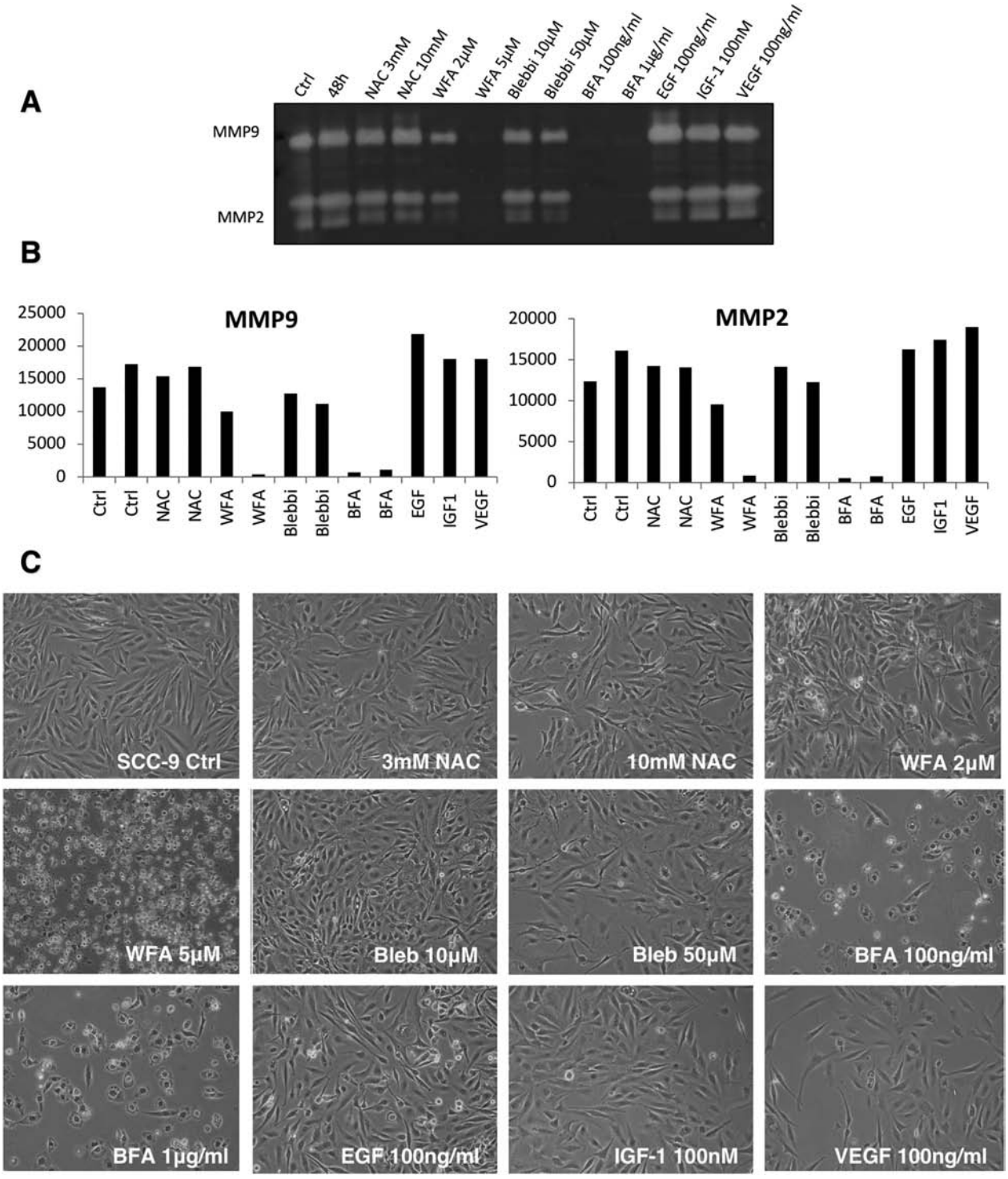

Figure 8. Evaluation of NMIIA's role in MMP9/2 secretion. A) SCC9 cells grown in SFM were treated with the inhibitor or growth factor indicated for 18 h. Aliquots of the conditioned medium were examined by in-gel zymography. B) Analysis of MMP2 and MMP9 secretion shown in A. C) Light microscopic examination of the cells treated as indicated in A. These data are representative of three independent experiments.

reported for a number of cell lines that were treated with blebbistatin or in which NMIIA was silenced [49].

NMIIA Participates in MMP Secretion

We next compared the effects of WFA (vimentin/NEDD9 inhibitor), blebbistatin (NMIIA inhibitor), the fungal metabolite Brefeldin A (BFA, blocks ER-to-Golgi transport; [50]) and the anti-oxidant N-acetyl-cysteine (NAC; control), on matrix metalloproteinase-9/2 (MMP9/2) secretion by SCC9 cells. MMP9 secretion is a key event in the invasive process [3] and we have shown that its secretion is required for cells to form invadopodia, the organelles that mediate cancer cell invasion [51] and which represent

the sites of focal secretion on of MMP9 by cancer cells [6]. The antioxidant NAC had no discernible effect on MMP secretion or SCC9 cell morphology (Figure 8, *A–C*), while EGF, IGF-1 and VEGF all had modest stimulatory actions on MMP secretion. Addition of blebbistatin preferentially inhibited MMP9 secretion over that of MMP-2. Addition of WFA (5 μM) completely inhibited secretion of both MMPs; at 2 μM it blocked MMP secretion by ~50% (Figure 8, *A* and *B*). This difference may be related to the number of functional cells capable of secretion in the presence of these two doses of drug and thus may be a reflection of WFA toxicity. Treatment of SCC9 cells with the Golgi transport disrupting agent and positive control, BFA [50,52] effectively blocked MMP9/2 secretion at both 100 ng/ml and 1 μg/ml doses, consistent with secretory pathway blockade inhibiting MMP secretion [53,54].

Discussion

Head and Neck cancer is the 6th most prevalent cancer worldwide [55], with NEDD9 playing a prominent role in its progression to an invasive, metastatic phenotype [3–6,56]. In the present studiy we identified vimentin and NMIIA as members of the NEDD9 interactome, participating in MMP secretion. Vimentin is a type III intermediate filament known for its role as a molecular marker of EMT [7,8]. To that end, we previously demonstrated that elevated NEDD9 levels promote EMT and using proximity ligation assays showed that MICAL1 and NEDD9 interact with vimentin [3–6,56]. These data support the notion that NEDD9, vimentin and their association may be part of a network involved in signaling to cell invasion, consistent with vimentin pushing cytoskeletal architecture to a more mesenchymal phenotype during EMT [15,26,38]. Additional support for this is provided by directly demonstrating that vimentin and NMIIA interact with NEDD9.

A role for vimentin in the invasive process has been described, based on its presence in maturing invadopodia [12,27] and mature pseudopodia [28,57]. Based on the premise that MMP release from cells occurs by its focal secretion at invadopodia in a NEDD9-dependent manner [3–6], we applied the use of WFA as a vimentin inhibitor in an effort to further test vimentin's role in MMP secretion. While our results did not support a role for WFA as a vimentin inhibitor; one of many actions attributed to WFA [58], we did observe an effect of WFA on NEDD9 levels. In cell fractionation analysis, we found that vimentin localizes to the cytoskeleton, where it co-immunoprecipitated with NEDD9. We were unable to demonstrate an interaction between vimentin and MICAl1 by immunoprecipitation, similar to our previous findings in which the interaction between these two proteins was only detectable by proximity ligation assay [3,6]. We noted a relationship between these two proteins whereby silencng MICAL1 resulted in reduced vimentin expression levels [3,6]. This was accompanied by a decrease in N-cadherin and an increase in E-cadherin levels, consistent with mesenchymal to epithelial transition (MET).

Vimentin phosphorylation regulates a number of cellular functions. For example, Ser71 phosphorylation was reported to stimulate vimentin filament formation during cytokinesis [59]. The NEDD9 paralog, p130Cas, was reported to be a vimentin interacting protein that is displaced from vimentin upon phosphorylation of Ser56 [46,47]. Our observation that vimentin present in immune precipitates of EGFP-NEDD9 is not phosphorylated at Ser56 suggests that NEDD9, similar to p130Cas, binds to unphosphorylated (Ser56) vimentin. This suggests that the constitutive phosphorylation seen at Ser56 occurs on vimentin that is not associated with NEDD9. Whether vimentin phosphorylation is required for MMP9 secretion in HNSCC cells not clear. In neutrophils, GTP induces Ser56 phosphorylation of vimentin via cyclin-dependent kinase 5, stimulating MMP9 secretion [60]. Consistent with our finding that NEDD9-bound vimentin is not phosphorylated at Ser56, WFA was reported to inhibit breast cancer cell invasion and metastasis by inducing Ser56 phosphorylation and vimentin disassembly [61]. Ser38 is another site of regulatory phosphorylation which has been shown to increase vimentin binding to α5β1 integrin [62]. In this context, inhibition of vimentin phosphorylation by pkCε inhibited endocytiosis of integrin-containing vesicles and cell haptotaxis [63]. Taken together, it is likely that phosphorylated and non-phosphorylated vimentin have roles in regulating MMP9 secretion, endocytic vesicle trafficking and cell architecture.

Identification of NMIIA as a NEDD9-interacting protein is consistent with its role in vesicular trafficking and MMP secretion [3–6]. NMIIA regulates mechanosensing, cell morphology, contributes to generating forces that alter cell signaling and regulates synaptic growth of neurons [18]. NMIIA has been shown to bind to Rab6 at the Golgi with blebbistatin treatment blocking fission of Rab6 transport carriers from the Golgi [29,64]. Related to this observation, we previously demonstrated that MICAL1 knockdown abrogates vimentin expression and leads to Rab6 accumulation and decreased MMP2/9 secretion [6]. Additional support for NMIIA having a role in secretion is based on the inhibition of MMP9 secretion following treatment of cells with the NMIIA-sepcific inbibitor, blebbistatin. This may reflect a block in vesicle trafficking in the secretory pathway downstream of NMIIA and Rab6 function at the Golgi where they direct vesicle trafficking from the ER to the Golgi and the plasma membrane [29,30].

NMIIA present in NEDD9 immunoprecipitates was phosphorylated on Ser1943. Ser1943 phosphorylation has been shown to block NMIIA filament formation and to enhance NMIIA binding to the cytoplasmic tails of Golgi glycosyl transferases [48]. Pasapera and coworkers [19] showed that NMIIA phosphorylation at Ser1916 increases its association with FAs, whereas Rai and coworkers found that Ser1943 phosphorylation also contributes to FA association and that mutation of either Ser 1916 or 1943 diminishes this association [65]. Other studies have suggested that NMIIA phosphorylation increases breast cancer cell migration rates [25]. It is notable that NEDD9 phosphorylation at its SD tyrosine residues appears to be required for NEDD9-NMIIA binding. Blebbistatin treatment reduced MMP secretion which may be attributable to reduced trafficking of MMP-containing vesicles from the Golgi complex for export from the cells [29,30]. Ivkovic and coworkers reported that NMIIA regulates glioma cell invasion in response to multiple signlaing pathways with blebbistatin inhibiting all pathways leading to Ser1943 phosphorylation [66]. Accordingly, they made the case that NMIIA is a valid therapeutic target for glioblastoma invasion. In the context of the current findings, NMIIA may also be a valid therapeutic target in HNSCC.

Conclusion

The cytoskeletal proteins vimentin and NMIIA are involved in numerous cellular activities including migration/invasion, secretion and cell morphology, many of which naturally intersect with those of

NEDD9. Given that NEDD9 is a member of the metastatic signature for a number of types of cancer, it is likley that vimentin and NMIIA will emerge as regulators of the invasive, metastatic phenotype.

Acknowledgments

The authors thank Jennifer Bethard for LC-MS/MS analysis of proteins Mass Spectrometry Facility, Department of Cell and Molecular Pharmacology and Experimental Therapeutics, MUSC, Charleston, SC. This work was supported, in part, by the shRNA, Flow Cytometry and Cell Sorting, Biostatistics, and Cell and Molecular Imaging Shared Resources, Hollings Cancer Center (HCC), Medical University of South Carolina (P30 CA138313). This work was supported by the following funding agencies: National Cancer Institute USA R01 CA134845 (SAR), P30 CA138313 (Hollings Cancer Center), 1K12 CA157588 (DMN), National Institute of Dental and Craniofacial Research 1K08 DE026542 (DMN). BrightFocus® Foundation USA grant #2009086 (SAR), Department of Defense USA award N6311601MD10004 (SAR). MS respectfully acknowledges support from the European Social Fund, grant project SOFOS-Knowledge and Skill Development of Staff of P. J. Šafárik University in Košice (contract number: 003/2013/1.2/OPV, ITMS code: 26110230088). PB was supported by the University Grants Council of India Raman Postdoctoral Fellowship Programme, F. No. 5-11/2013(IC) dated 27-08-2014.

References

[1] Kim M, Gans JD, Nogueira C, Wang A, Paik JH, Feng B, Brennan C, Hahn WC, Cordon-Cardo C, and Wagner SN, et al (2006). Comparative oncogenomics identifies NEDD9 as a melanoma metastasis gene. *Cell* **125**, 1269–1281.

[2] Singh MK, Izumchenko E, Klein-Szanto AJ, Egleston BL, Wolfson M, and Golemis EA (2010). Enhanced genetic instability and dasatinib sensitivity in mammary tumor cells lacking NEDD9. *Cancer Res* **70**, 8907–8916.

[3] Lucas Jr JT, Salimath BP, Slomiany MG, and Rosenzweig SA (2010). Regulation of invasive behavior by vascular endothelial growth factor is HEF1-dependent. *Oncogene* **29**, 4449–4459.

[4] Loudig O, Brandwein-Gensler M, Kim RS, Lin J, Isayeva T, Liu C, Segall JE, Kenny PA, and Prystowsky MB (2011). Illumina whole-genome complementary DNA-mediated annealing, selection, extension and ligation platform: assessing its performance in formalin-fixed, paraffin-embedded samples and identifying invasion pattern-related genes in oral squamous cell carcinoma. *Hum Pathol* **42**, 1911–1922.

[5] Sima N, Cheng X, Ye F, Ma D, Xie X, and Lu W (2013). The overexpression of scaffolding protein NEDD9 promotes migration and invasion in cervical cancer via tyrosine phosphorylated FAK and SRC. *PLoS One* **8**e74594.

[6] Grauzam S, Brock AM, Holmes CO, Tiedeken JA, Boniface SG, Pierson BN, Patterson DG, Coaxum SD, Neskey DM, and Rosenzweig SA (2018). NEDD9 stimulated MMP9 secretion is required for invadopodia formation in oral squamous cell carcinoma. *Oncotarget* **9**, 25503–25516.

[7] Thiery JP, Acloque H, Huang RY, and Nieto MA (2009). Epithelial-mesenchymal transitions in development and disease. *Cell* **139**, 871–890.

[8] Jin Y, Li F, Zheng C, Wang Y, Fang Z, Guo C, Wang X, Liu H, Deng L, and Li C, et al (2014). NEDD9 promotes lung cancer metastasis through epithelial-mesenchymal transition. *Int J Cancer* **134**, 2294–2304.

[9] Takkunen M, Grenman R, Hukkanen M, Korhonen M, Garcia de Herreros A, and Virtanen I (2006). Snail-dependent and -independent Epithelial-Mesenchymal Transition in Oral Squamous Carcinoma Cells. *J Histochem Cytochem* **54**, 1263–1275.

[10] de Araujo VC, Pinto Junior DS, de Sousa SO, Nunes FD, and de Araujo NS (1993). Vimentin in oral squamous cell carcinoma. *Eur Arch Otorhinolaryngol* **250**, 105–109.

[11] Balasundaram P, Singh MK, Dinda AK, Thakar A, and Yadav R (2014). Study of beta-catenin, E-cadherin and vimentin in oral squamous cell carcinoma with and without lymph node metastases. *Diagn Pathol* **9**, 145.

[12] Eriksson JE, Dechat T, Grin B, Helfand B, Mendez M, Pallari HM, and Goldman RD (2009). Introducing intermediate filaments: from discovery to disease. *J Clin Invest* **119**, 1763–1771.

[13] Islam S, Kim JB, Trendel J, Wheelock MJ, and Johnson KR (2000). Vimentin expression in human squamous carcinoma cells: relationship with phenotypic changes and cadherin-based cell adhesion. *J Cell Biochem* **78**, 141–150.

[14] Tanaka N, Odajima T, Ogi K, Ikeda T, and Satoh M (2003). Expression of E-cadherin, alpha-catenin, and beta-catenin in the process of lymph node metastasis in oral squamous cell carcinoma. *Br J Cancer* **89**, 557–563.

[15] Satelli A and Li S (2011). Vimentin in cancer and its potential as a molecular target for cancer therapy. *Cell Mol Life Sci* **68**, 3033–3046.

[16] Matveeva EA, Venkova LS, Chernoivanenko IS, and Minin AA (2015). Vimentin is involved in regulation of mitochondrial motility and membrane potential by Rac1. *Biol Open* **4**, 1290–1297.

[17] Heissler SM and Manstein DJ (2013). Nonmuscle myosin-2: mix and match. *Cell Mol Life Sci* **70**, 1–21.

[18] Newell-Litwa KA, Horwitz R, and Lamers ML (2015). Non-muscle myosin II in disease: mechanisms and therapeutic opportunities. *Dis Model Mech* **8**, 1495–1515.

[19] Pasapera AM, Plotnikov SV, Fischer RS, Case LB, Egelhoff TT, and Waterman CM (2015). Rac1-dependent phosphorylation and focal adhesion recruitment of myosin IIA regulates migration and mechanosensing. *Curr Biol* **25**, 175–186.

[20] Golomb E, Ma X, Jana SS, Preston YA, Kawamoto S, Shoham NG, Goldin E, Conti MA, Sellers JR, and Adelstein RS (2004). Identification and characterization of nonmuscle myosin II-C, a new member of the myosin II family. *J Biol Chem* **279**, 2800–2808.

[21] Leal A, Endele S, Stengel C, Huehne K, Loetterle J, Barrantes R, Winterpacht A, and Rautenstrauss B (2003). A novel myosin heavy chain gene in human chromosome 19q13.3. *Gene* **312**, 165–171.

[22] Toothaker LE, Gonzalez DA, Tung N, Lemons RS, Le Beau MM, Arnaout MA, Clayton LK, and Tenen DG (1991). Cellular myosin heavy chain in human leukocytes: isolation of 5' cDNA clones, characterization of the protein, chromosomal localization, and upregulation during myeloid differentiation. *Blood* **78**, 1826–1833.

[23] Simons M, Wang M, McBride OW, Kawamoto S, Yamakawa K, Gdula D, Adelstein RS, and Weir L (1991). Human nonmuscle myosin heavy chains are encoded by two genes located on different chromosomes. *Circ Res* **69**, 530–539.

[24] Arozarena I, Sanchez-Laorden B, Packer L, Hidalgo-Carcedo C, Hayward R, Viros A, Sahai E, and Marais R (2011). Oncogenic BRAF induces melanoma cell invasion by downregulating the cGMP-specific phosphodiesterase PDE5A. *Cancer Cell* **19**, 45–57.

[25] Dulyaninova NG and Bresnick AR (2013). The heavy chain has its day: regulation of myosin-II assembly. *BioArchitecture* **3**, 77–85.

[26] Liu CY, Lin HH, Tang MJ, and Wang YK (2015). Vimentin contributes to epithelial-mesenchymal transition cancer cell mechanics by mediating cytoskeletal organization and focal adhesion maturation. *Oncotarget* **6**, 15966–15983.

[27] Schoumacher M, Goldman RD, Louvard D, and Vignjevic DM (2010). Actin, microtubules, and vimentin intermediate filaments cooperate for elongation of invadopodia. *J Cell Biol* **189**, 541–556.

[28] Mimae T and Ito A (2015). New challenges in pseudopodial proteomics by a laser-assisted cell etching technique. *Biochim Biophys Acta* **1854**, 538–546.

[29] Miserey-Lenkei S, Chalancon G, Bardin S, Formstecher E, Goud B, and Echard A (2010). Rab and actomyosin-dependent fission of transport vesicles at the Golgi complex. *Nat Cell Biol* **12**, 645–654.

[30] Miserey-Lenkei S, Bousquet H, Pylypenko O, Bardin S, Dimitrov A, Bressanelli G, Bonifay R, Fraisier V, Guillou C, and Bougeret C, et al (2017). Coupling fission and exit of RAB6 vesicles at Golgi hotspots through kinesin-myosin interactions. *Nat Commun* **8**, 1254.

[31] Schramek D, Sendoel A, Segal JP, Beronja S, Heller E, Oristian D, Reva B, and Fuchs E (2014). Direct in vivo RNAi screen unveils myosin IIa as a tumor suppressor of squamous cell carcinomas. *Science* **343**, 309–313.

[32] Coaxum SD, Tiedeken J, Garrett-Mayer E, Myers J, Rosenzweig SA, and Neskey DM (2017). The tumor suppressor capability of p53 is dependent on non-muscle myosin IIA function in head and neck cancer. *Oncotarget* **8**, 22991–23007.

[33] Lin CJ, Grandis JR, Carey TE, Gollin SM, Whiteside TL, Koch WM, Ferris RL, and Lai SY (2007). Head and neck squamous cell carcinoma cell lines: established models and rationale for selection. *Head Neck* **29**, 163–188.

[34] Azar WJ, Zivkovic S, Werther GA, and Russo VC (2014). IGFBP-2 nuclear translocation is mediated by a functional NLS sequence and is essential for its pro-tumorigenic actions in cancer cells. *Oncogene* **33**, 578–588.

[35] Slomiany MG, Black LA, Kibbey MM, Day TA, and Rosenzweig SA (2006). IGF-1 induced vascular endothelial growth factor secretion in head

and neck squamous cell carcinoma. *Biochem Biophys Res Commun* **342**, 851–858.

[36] Hong K-O, Kim J-H, Hong J-S, Yoon H-J, Lee J-I, Hong S-P, and Hong S-D (2009). Inhibition of Akt activity induces the mesenchymal-to-epithelial reverting transition with restoring E-cadherin expression in KB and KOSCC-25B oral squamous cell carcinoma cells. *J Exp Clin Cancer Res* **28**, 28.

[37] Shi AM, Tao ZQ, Li R, Wang YQ, Wang X, and Zhao J (2016). Vimentin and post-translational modifications in cell motility during cancer - a review. *Eur Rev Med Pharmacol Sci* **20**, 2603–2606.

[38] Mendez MG, Kojima S, and Goldman RD (2010). Vimentin induces changes in cell shape, motility, and adhesion during the epithelial to mesenchymal transition. *FASEB J* **24**, 1838–1851.

[39] de Andrade NP, Rodrigues MF, Rodini CO, and Nunes FD (2017). Cancer stem cell, cytokeratins and epithelial to mesenchymal transition markers expression in oral squamous cell carcinoma derived from ortothopic xenoimplantation of CD44(high) cells. *Pathol Res Pract* **213**, 235–244.

[40] Hivert V, Pierre J, and Raingeaud J (2009). Phosphorylation of human enhancer of filamentation (HEF1) on serine 369 induces its proteasomal degradation. *Biochem Pharmacol* **78**, 1017–1025.

[41] Suzuki T, Nakamoto T, Ogawa S, Seo S, Matsumura T, Tachibana K, Morimoto C, and Hirai H (2002). MICAL, a novel CasL interacting molecule, associates with vimentin. *J Biol Chem* **277**, 14933–14941.

[42] Shaiken TE and Opekun AR (2014). Dissecting the cell to nucleus, perinucleus and cytosol. *Sci Rep* **4**, 4923.

[43] Bargagna-Mohan P, Hamza A, Kim YE, Khuan Abby Ho Y, Mor-Vaknin N, Wendschlag N, Liu J, Evans RM, Markovitz DM, and Zhan CG, et al (2007). The tumor inhibitor and antiangiogenic agent withaferin A targets the intermediate filament protein vimentin. *Chem Biol* **14**, 623–634.

[44] Piatkov KI, Brower CS, and Varshavsky A (2012). The N-end rule pathway counteracts cell death by destroying proapoptotic protein fragments. *Proc Natl Acad Sci U S A* **109**, E1839-1847.

[45] Ivaska J, Pallari HM, Nevo J, and Eriksson JE (2007). Novel functions of vimentin in cell adhesion, migration, and signaling. *Exp Cell Res* **313**, 2050–2062.

[46] Li QF, Spinelli AM, Wang R, Anfinogenova Y, Singer HA, and Tang DD (2006). Critical role of vimentin phosphorylation at Ser-56 by p21-activated kinase in vimentin cytoskeleton signaling. *J Biol Chem* **281**, 34716–34724.

[47] Wang R, Li QF, Anfinogenova Y, and Tang DD (2007). Dissociation of Crk-associated substrate from the vimentin network is regulated by p21-activated kinase on ACh activation of airway smooth muscle. *Am J Physiol Lung Cell Mol Physiol* **292**, L240–L248.

[48] Petrosyan A, Ali MF, Verma SK, Cheng H, and Cheng PW (2012). Non-muscle myosin IIA transports a Golgi glycosyltransferase to the endoplasmic reticulum by binding to its cytoplasmic tail. *Int J Biochem Cell Biol* **44**, 1153–1165.

[49] Chen G, Hou Z, Gulbranson DR, and Thomson JA (2010). Actin-myosin contractility is responsible for the reduced viability of dissociated human embryonic stem cells. *Cell Stem Cell* **7**, 240–248.

[50] Klausner RD, Donaldson JG, and Lippincott-Schwartz J (1992). Brefeldin A: insights into the control of membrane traffic and organelle structure. *J Cell Biol* **116**, 1071–1080.

[51] Jacob A and Prekeris R (2015). The regulation of MMP targeting to invadopodia during cancer metastasis. *Front Cell Dev Biol* **3**, 4.

[52] Nebenfuhr A, Ritzenthaler C, and Robinson DG (2002). Brefeldin A: deciphering an enigmatic inhibitor of secretion. *Plant Physiol* **130**, 1102–1108.

[53] Sbai O, Ferhat L, Bernard A, Gueye Y, Ould-Yahoui A, Thiolloy S, Charrat E, Charton G, Tremblay E, and Risso JJ, et al (2008). Vesicular trafficking and secretion of matrix metalloproteinases-2, -9 and tissue inhibitor of metalloproteinases-1 in neuronal cells. *Mol Cell Neurosci* **39**, 549–568.

[54] Tseng CN, Huang CF, Cho CL, Chang HW, Huang CW, Chiu CC, and Chang YF (2013). Brefeldin a effectively inhibits cancer stem cell-like properties and MMP-9 activity in human colorectal cancer Colo 205 cells. *Molecules* **18**, 10242–10253.

[55] Day TA, Davis BK, Gillespie MB, Joe JK, Kibbey M, Martin-Harris B, Neville B, Richardson MS, Rosenzweig S, and Sharma AK, et al (2003). Oral cancer treatment. *Curr Treat Options in Oncol* **4**, 27–41.

[56] Grauzam S, Brock AM, Holmes CO, Tiedeken JA, Boniface SG, Pierson BN, Patterson DG, Coaxum SD, Neskey DM, and Rosenzweig SA (2018). NEDD9 stimulated MMP9 secretion is required for invadopodia formation in oral squamous cell carcinoma. *Oncotarget* **9**, 25503–25516.

[57] Havrylov S and Park M (2015). MS/MS-based strategies for proteomic profiling of invasive cell structures. *Proteomics* **15**, 272–286.

[58] Vanden Berghe W, Sabbe L, Kaileh M, Haegeman G, and Heyninck K (2012). Molecular insight in the multifunctional activities of Withaferin A. *Biochem Pharmacol* **84**, 1282–1291.

[59] Li Z, Li X, Nai S, Geng Q, Liao J, Xu X, and Li J (2017). Checkpoint kinase 1-induced phosphorylation of O-linked beta-N-acetylglucosamine transferase regulates the intermediate filament network during cytokinesis. *J Biol Chem* **292**, 19548–19555.

[60] Lee KY, Liu L, Jin Y, Fu SB, and Rosales JL (2012). Cdk5 mediates vimentin Ser56 phosphorylation during GTP-induced secretion by neutrophils. *J Cell Physiol* **227**, 739–750.

[61] Thaiparambil JT, Bender L, Ganesh T, Kline E, Patel P, Liu Y, Tighiouart M, Vertino PM, Harvey RD, and Garcia A, et al (2011). Withaferin A inhibits breast cancer invasion and metastasis at sub-cytotoxic doses by inducing vimentin disassembly and serine 56 phosphorylation. *Int J Cancer* **129**, 2744–2755.

[62] Kim J, Jang J, Yang C, Kim EJ, Jung H, and Kim C (2016). Vimentin filament controls integrin alpha5beta1-mediated cell adhesion by binding to integrin through its Ser38 residue. *FEBS Lett* **590**, 3517–3525.

[63] Ivaska J, Vuoriluoto K, Huovinen T, Izawa I, Inagaki M, and Parker PJ (2005). PKCepsilon-mediated phosphorylation of vimentin controls integrin recycling and motility. *EMBO J* **24**, 3834–3845.

[64] Petrosyan A (2015). Onco-Golgi: Is fragmentation a gate to cancer progression? *Biochem Mol Biol J* **1**.

[65] Rai V, Thomas DG, Beach JR, and Egelhoff TT (2017). Myosin IIA Heavy Chain Phosphorylation Mediates Adhesion Maturation and Protrusion in Three Dimensions. *J Biol Chem* **292**, 3099–3111.

[66] Ivkovic S, Beadle C, Noticewala S, Massey SC, Swanson KR, Toro LN, Bresnick AR, Canoll P, and Rosenfeld SS (2012). Direct inhibition of myosin II effectively blocks glioma invasion in the presence of multiple motogens. *Mol Biol Cell* **23**, 533–542.

[67] Matsuyama M, Tanaka H, Inoko A, Goto H, Yonemura S, Kobori K, Hayashi Y, Kondo E, Itohara S, and Izawa I, et al (2013). Defect of mitotic vimentin phosphorylation causes microophthalmia and cataract via aneuploidy and senescence in lens epithelial cells. *J Biol Chem* **288**, 35626–35635.

[68] Dulyaninova NG, Malashkevich VN, Almo SC, and Bresnick AR (2005). Regulation of myosin-IIA assembly and Mts1 binding by heavy chain phosphorylation. *Biochemistry* **44**, 6867–6876.